THOMSON SCATTERING SYSTEMS FOR TURBULENT PLASMA DIAGNOSTICS

MURAOKA, Katsunori
Research Institute for Applied Mechanics, Kyushu University : Associate Professor

MITARAI, Osamu
Kyushu University : Graduate Student

GOTO, Seiichi
Plasma Physics Laboratory, Faculty of Engineering, Osaka University

SATOMI, Norio
Plasma Physics Laboratory, Faculty of Engineering, Osaka University

他

https://doi.org/10.5109/7173499

出版情報：Reports of Research Institute for Applied Mechanics. 22 (70), pp.165-175, 1975. 九州大学応用力学研究所
バージョン：

Reports of Research Institute for Applied Mechanics
Vol. XXII, No. 70, 1975

THOMSON SCATTERING SYSTEMS FOR TURBULENT PLASMA DIAGNOSTICS

By Katsunori MURAOKA*, Osamu MITARAI**,
Seiichi GOTO***, Norio SATOMI***,
Harukazu IGUCHI****, and Takaya KAWABE****

Two systems of Thomson scattering of ruby laser light are described, one for the PIACE (Plasma Injection And Compression Experiment) at the Plasma Physics Laboratory, Osaka University, and the other for THE Mach II (Turbulent Heating Experiment MACHine II) at the Institute of Plasma Physics, Nagoya University, both being designed to measure the electron temperature and density (or the electron velocity distribution function itself) and possibly the electron drift velocity of turbulently heated plasmas as functions of space and time. Some preliminary results are given.

1. Introduction

Although the laser scattering technique for plasma diagnostics has been developed since the laser iself was invented in 1960, the dramatic success of the method on a Tokamak by British physicists[1] has established it as one of the indispensable means to measure the electron temperature T_e and density n_e with good spatial and temporal resolutions. In recent years, there have been a number of proposals and actual measurements of various parameters of plasmas by means of the laser scattering technique besides T_e and n_e. These include the measurements of the turbulence spectrum[2),3)], the ion temperature[4)], the magnetic field intensity[5)], the electric current density distribution in a plasma[6),7)], the impurity concentration[8)], and others.

We have applied the well established method of measuring T_e and n_e onto two turbulently heated plasmas (in PIACE and THE Mach II), and the systems and some preliminary results are presented in this paper.

An infrared laser scattering system has now been developed by authors[9)], and its application to measurements of turbulence and/or ion temperature and impurity concentrations in these two devices will be tried in the near future.

* Associate Professor, Research Institute for Applied Mechanics, Kyushu University.
** Graduate Student, Kyushu University.
*** Plasma Physics Laboratory, Faculty of Engineering, Osaka University, Suita, Osaka.
**** Institute of Plasma Physics, Nagoya University, Nagoya.

2. Principle of the method

The principle of the laser scattering is now well known [10], and here the brief summary is presented only to introduce the nomenclatures in the later sections. In the vector diagram of Fig. 1, $\vec{k}_i$ is the incident-beam wave vector whose intensity is denoted by I_i, $\vec{k}_s$ the scattered-light wave vector (intensity I_s, $|\vec{k}_s|=|\vec{k}_i|$), and $\vec{k}$ the differential scattering vector ($k\equiv|\vec{k}|=2(\omega_0/c)\sin\theta/2$). Then, the differential scattering cross section $\sigma(\vec{k},\omega)$ can be defined by

$$I_s(\vec{k},\omega)d\omega d\Omega=I_iN_e\sigma(\vec{k},\omega)d\omega d\Omega \qquad (1)$$

where $d\omega$ is the frequency interval, $d\Omega$ the element of solid angle, and N_e the total number of scattering electrons.

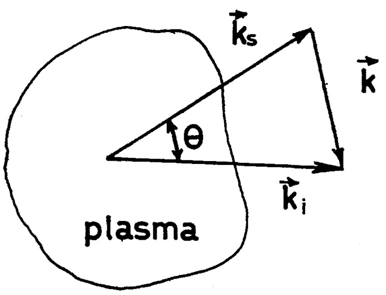

Fig. 1. Vector diagram defining the scattering geometry.

The dynamic form factor $S(\vec{k},\omega)$ is defined by using the Thomson cross section $\sigma_T=(e^2/m_ec^2)\sin^2\beta$ (e is the electronic charge, c the velocity of light and β the angle between the direction of observation from the scattering volume and the direction of the electric field of the incident laser light) as follows,

$$S(\vec{k},\omega)=\sigma(\vec{k},\omega)/\sigma_T \qquad (2)$$

The relative shape of $S(\vec{k},\omega)$ is completely determined by the factor $\alpha\equiv1/k\lambda_D$ for the thermal fluctuation of plasmas where λ_D is the electron Debye length.

For the present purpose, $\alpha\ll1$ is enough to be considered, and for this case,

$$S(\vec{k},\omega)=f_e\left(\frac{\omega_0-\omega}{k}\right) \qquad (3)$$

where f_e is the electron distribution function for the component of velocity along $\vec{k}$ normalized to the total number of electrons N_e and ω_0 is the incident laser light frequency. Equation (3) reduces to the following expression for the electron Maxwell distribution,

$$S(\vec{k}, \omega)=\left(\frac{1}{\pi^{1/2}kv_e}\right)\exp\left[-\left(\frac{\omega-\omega_0}{kv_e}\right)^2\right] \tag{4}$$

where

$$v_e=(2\kappa T_e/m_e)^{1/2} \tag{5}$$

or in the wavelength presentation

$$S(\vec{k}, \lambda)=\left(\frac{1}{\pi^{1/2}kv_e}\right)\exp\left[-\left\{\frac{2\pi c}{kv_e\lambda_0^2}(\lambda-\lambda_0)\right\}^2\right] \tag{6}$$

where λ_0 is the incident laser wavelength.

Equation (4) or (6) shows that by measuring the spectral shape of S, we can obtain the electron temperature T_e. For 90° scattering which is adopted for both of the present experiments, and for ruby laser wavelength (λ_0=6943 Å), T_e can be obtaind by knowing the 1/e intensity point of the scattered signal from Eq. (6) as follows,

$$\Delta\lambda_{1/e}(\text{Å})=19.3\sqrt{T_e(ev)} \tag{7}$$

Equation (1) shows that the measurement of the intensity of the scattered light I_s gives the number of scattering electrons N_e which in turn gives the electron density through a proper calibration procedure (e.g., by using the Rayleigh scattering from a neutral gas of known density).

3. System for the PIACE

3.1. PIACE

The details of the PIACE are described elsewhere [11], but it is essentially a fast linear θ pinch plasma heating experiment, the novel feature being that the initial plasma is produced by collisions of two counterstreaming plasmas. By this method of the initial plasma production, the parameters of the initial plasma can be varied over a wide range (e.g., $T_e \gtreqless T_i$) according as the selection of the delay of the θ pinch firing relative to the timing of the collision of the plasma streams.

Quite high values of both electron and ion temperatures have been obtained ($T\simeq T_i\simeq 4$ *kev*) for all the initial conditions tried, and it is the purpose of the subsequent experiments to clarify the heating mechanisms and possibly apply them to the next stage of the thermonuclear fusion researches. The Thomson scattering of ruby laser light has recently been added as one of the most important diagnostics to measure the temporal and spatial evolutions of the electron temperature and density, and possibly the electron drift velocity at the θ current layer.

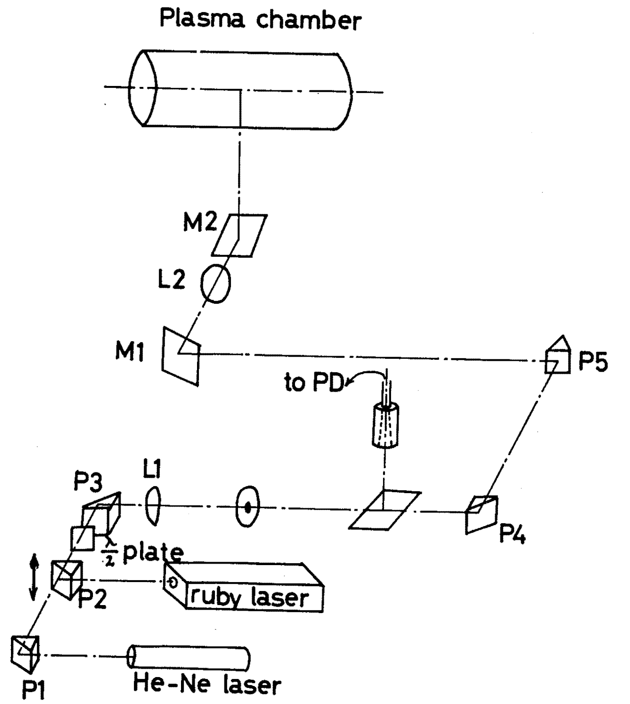

Fig. 2. Laser input optical arrangement for the PIACE experiment.

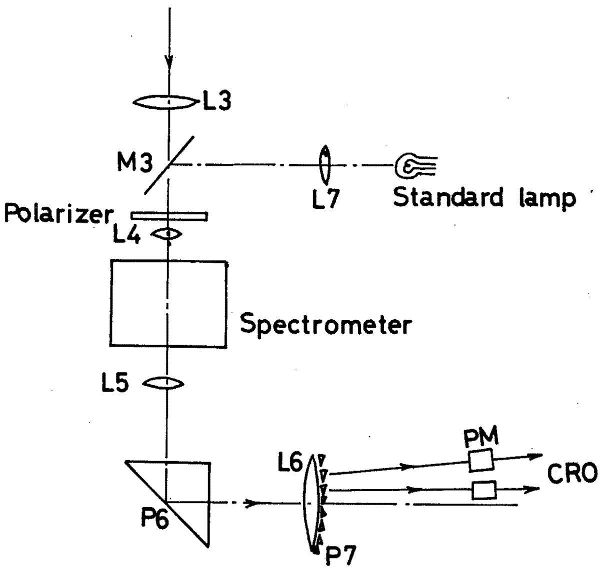

Fig. 3. Scattered light detection arrangement for the PIACE experiment.

3.2. Laser scattering system

The laser input optical system is shown in Fig. 2 and the collection optics of the scattered light in Fig. 3. Both of these optical systems as well as the laser are mounted onto a single bench and three-dimensional traverses of the system are possible with the whole optical system stayed aligned.

The main ratings and characteristics of the laser input optical system are as follows: the output of the ruby laser is 1 *J* in 20 *ns* (50 *MW*) with the beam divergence of 5 *mrad*, He-Ne laser beam being aligned with the path of the ruby laser light and used for the alignment of the whole system; the focal length of the input optics is 100 *mm* by the combination of lenses L1 and L2 and the beam spot size at the focal point is 1 *mm* ϕ; all the prisms, mirrors and lenses in Fig. 2 are anti-reflection coated giving the overall transmission of 80 %.

The scattered light optical system has the following characteristics: the spectrometer is of the Czerny-Turner mounting with $F=5.5$, $f=300$ *mm* and ruling of 1200 *lines/mm*; the multichannel optical system consists of two relay lenses (L5 and L6 in Fig. 2) and the small prisms P7 for separating the light path, and the relay lenses L5 and L6 can be interchanged with the other two spare sets to give the overall spectrum coverages of 200, 400 and 800 Å; the photomultiplier tubes are of RCA 7265 type (photocathode S-20); the scattered light optical system has such accessories as the standard lamp for the calibration of the system, the delay cables with the time delay of the successive channel of 50 *ns* for facilitating the tracing of all the eight channels onto one oscilloscope, signal filters (10 *MHz*~1 *GHz*), signal attenuators (~1 *GHz*), and the signal amplifiers (10 *dB*).

3.3. Results

One of the typical results is shown in Fig. 4 in which, from Eq. (6), the relative intensity of the scattered light is plotted against $(\lambda-\lambda_0)^2$, the data well approximated by a straight line showing the Maxwell distribution of electrons to be well satisfied. The measurement is done on the axis and at the midplane of the discharge tube about 1 μs after the θ pinch compression firing (the rise time of the compression field is 1.4 μs). The initial plasma parameters before the compression are $n_e \simeq 5\times10^{20} m^{-3}$, $T_e=15$ *ev* and $T_i \sim 100$ *ev*. The timing of the laser firing has been varied over 0.5~1.5 μs after the start of the compression but the measured temperatures varies only from 180 to 250 *ev*. The previous measurements of the electron temperature by the soft x-ray absorption method[11] have given $T_e \sim 4$ *kev* for the same experimental condition. One possible explanation of the discrepancy between these two results can be that the initial plasma may have been changed after the repair of the machine subsequent to the initial experiments which lasted until the end of 1972, in which the soft x-ray measurement was done, and the heating mechanisms may be different for the two initial conditions of the plasma realized. One indication to support this explanation is that the

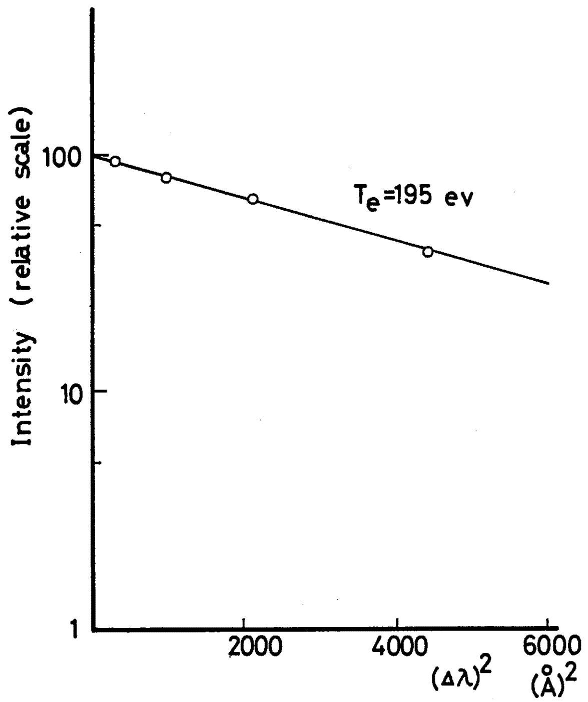

Fig. 4. Scattered light intensities against the wavelength differences from the ruby laser wavelength squared.

electron density on the axis of the discharge tube measured by the laser scattering after the compression ($\sim 8\times10^{21}m^{-3}$) seems to be much higher than the results of the previous measurements by the absolute intensity of continuum($\sim 9\times10^{20}m^{-3}$). But a more likely explanation can be that the electron distibution may not be a single Maxwellian and the high energy component of the electron velocity distribution heavily contributes the soft x-ray radiation, whereas the laser scattering gives the information about the distribution of the bulk of the electrons.

These points will be clarified by changing the parameters of the initial plasma and by more detailed measurements, in particular by the simultaneous measurements of the soft x-ray radiation and the laser scattering.

4. System for the Mach II

4.1. The Mach II

The Mach II is a linear z discharge machine in which a large axial current is induced in a plasma, which drives the turbulence and the turbulence in turn heats the plasma by the interaction of the current with the turbu-

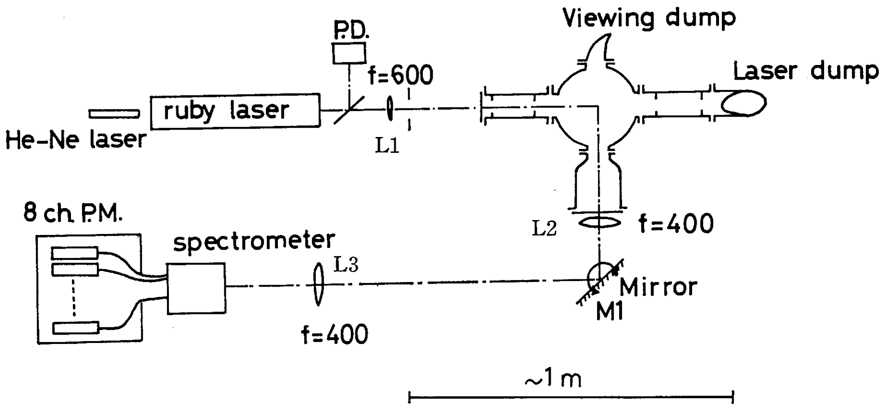

Fig. 5. Schematic arrangement of the equipments of the scattering experiment for THE Mach II.

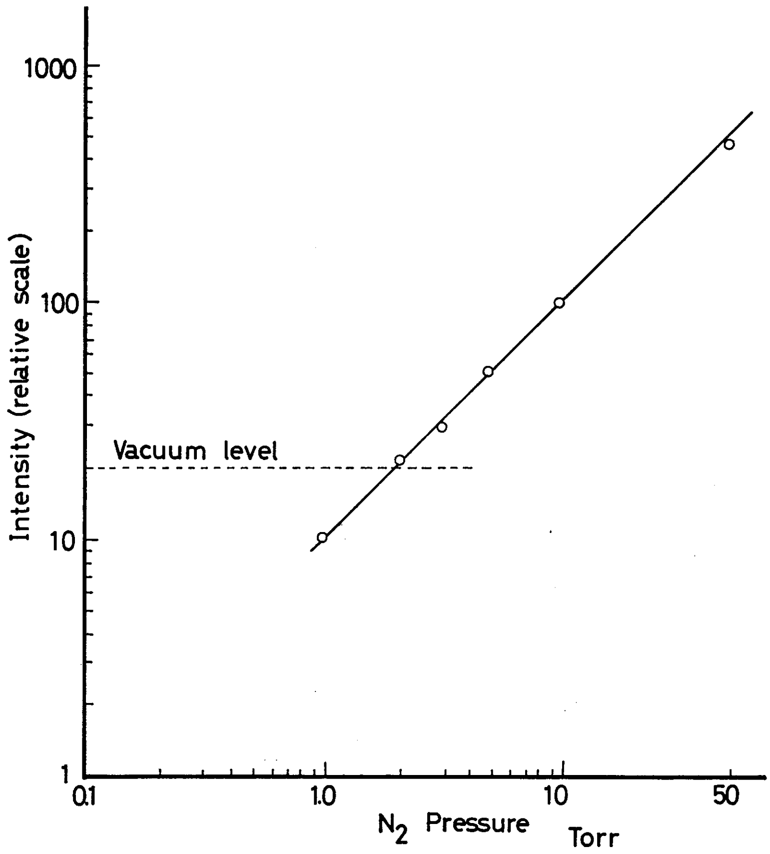

Fig. 6. Rayleigh scattering from a nitrogen gas.

lence. The initial plasma flows freely from a Titanium washer gun to a strong magnetic field (up to 25 *kG*) with a mirror configuration. The details of the apparatus and the dynamic behaviour of the plasma are described elsewhere [12]. Strong electron and ion heating up to several *kev* have been observed after about 1 μs from the initiation of the z-discharge and it is the task of the ruby laser scattering to measure the spatial and temporal evolution of the electron density, temperature and drift velocity.

4.2. Laser scattering system

The arrangement of the experimental equipments is shown in Fig. 5, in which a more powerful laser (10 *J* in 20 *ns* giving 500 *MW*) than in the case of the PIACE has been used to measure at a lower density ($\simeq 10^{18} \sim 10^{19}\ m^{-3}$) and about the same temperature. A single focussing lens L1 is used for simplicity and it has been working well. In the optical system of the scattered light, the tilting of a mirror M1 gives the radial scan of the point of observation, the light from which is focussed onto the input port of the spectrometer. The spectometer is NIKON P-250 having the dispersion of 30 Å/*mm*. The light at the exit of the spectrometer is lead to the input ports of the 8 channel photomultiplier tubes (RCA 7265) through light guides. The signals are then fed through preamplifiers into oscilloscopes.

4.3. Results

One of the typical results of the Rayleigh sattering from nitrogen gas is shown in Fig. 6. The stray light level is 2 *mTorr* N_2 equivalent which corresponds to the electron density of about $10^{20}\ m^{-3}$. Because of this rather

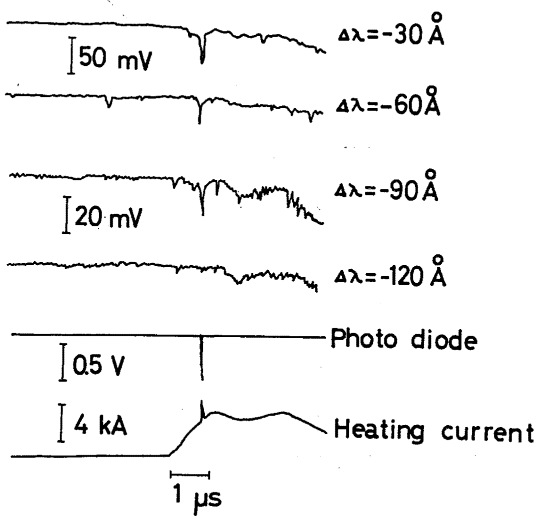

Fig. 7. Typical scattered light signals.

high stray light level, it has not been possible to use the photomultiplier tube at the laser wavelength.

One typical result of Thomson scattering signals is shown in Fig. 7 for the initial plasma of $n_e \simeq 10^{19}\ m^{-3}$ and $T_e \simeq 10\ ev$. The charging voltage of the heating bank (for z-discharge)is 30 *kV* and the magnetic flux with the mirror configuration 0.65 *Tesla* at the centre of the discharge tube (mirror ratio 2). The bottom trace of Fig. 7 shows the heating current added by the photodiode output to know the timing of the laser firing relative to the heating current.

By doing the similar experiments at different times of the heating cur-

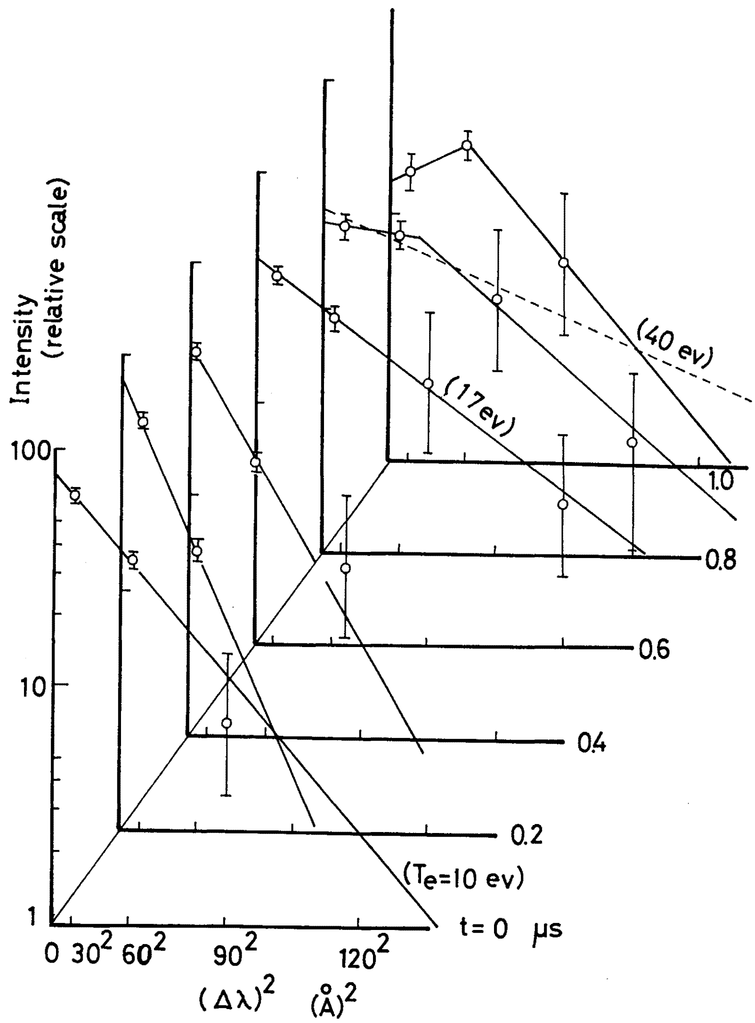

Fig. 8 Time evolution of the scattered light intensities.

rent, and by using the results of the responce calibration of the light-guide photomultiplier tube system, we get the result of Fig. 8, in which, following Eq. (6) as before, the logarithm of the scattered intensity at each channel (x-axis) has been plotted against the wavelength separation from the laser wavelength squared (y-axis), and z-axis shows the time from the initiation of the heating current. The electron temperatures obtained from the slopes of the data are shown in the figure. The electron density has been obtained by integrating the intensity distribution and by using the result of the Rayleigh scattering in Fig. 6 to get 5×10^{18} m^{-3} at $t=0$ and remained almost constant during the measurements (up to $t=1.0$ μs).

The main results obtained so far are; i) the initial temperature is 10 *ev* and remains almost at this value after 0.1~0.15 μs from the initiation of the heating discharge, ii) at about $t=0.2$ μs, the temperature once drops to 5~6 *ev* and stays there for $0.2\lesssim t\lesssim 0.6$ μs, iii) from $t\simeq 0.6$ μs, T_e increases to about 50 *ev* at $t\simeq 0.8$ μs, iv) from $t\simeq 0.8$ μs, the electron distribution exhibits a marked deviation from the Maxwellian as seen in the plots at $t=0.8$ and 1.0 μs of Fig. 8, but these are not very reproducible, and v) the scattered signals are not observed after $t\simeq 1.2$ μs.

The cause of the observation ii) is not yet known but one possible explanation[13] could be that there is an axial distribution of the electron temperature and the cold electrons nearer to the electrode flow to the region of observation after sometime (~0.2 μs) from the initiation of the heating discharge. Subsequently, the electron heating follows by the classical and/or anomalous Joule dissipation as observed in iii). The causes of the observations iv) and v) are again unknown, but it could be due to the fact that the bulk of the plasma moves (the direction and the time of the movement could be irreproducible) and the dip in the distribution function at the laser wavelength at $t=0.8$ and 1.0 μs in Fig. 8 is due to the Doppler shift relative to the scattering vector $\vec{k}$ and subsequently the plasma escapes from the observation region as seen in v).

It must be stressed that these explanations are only tentative and different reasonings can not be excluded.

5. Discussion

It has been the purpose of this report to show that the two systems have actually started to work. There are several points of improvements found in the course of the experiments, e.g., the divergence of the laser beam (5~7 *mrad*) has been found to be larger than that expected (3 *mrad*) and consequently the optical system has to be modified, the delay and gating systems have not been used because of the overlapping of the background plasma radiation of all channels (by a poor gating) and the output signal of each channel has to be supplied directly to the oscilloscope, and the calibrations of the detection systems are not yet fully undertaken.

These points will be cleared in the near future and the systems are expected to give important informations for the clarifications of the heating mechanisms of the PIACE and THE Mach II experiments.

A part of the PIACE experiment has been supported by the Grant-in-Aid for the Scientific Researches from the Ministry of Education and THE Mach II experiment has been done through the collaborating research programmes at the Institute of Plasma Physics, Nagoya University.

References

1) Peacock, N. J. et al, Nature Vol. 224, 1969, p. 488.
2) Daughney, C.C., Holmes, L.S., and Paul, J.W.M., Phys. Rev. Lett. Vol. 25, 1970, p. 497.
3) Muraoka, K., Paul, J.W.M., and Daughney, C.C., Rep. Res. Inst. Appl. Mech. Vol. XXII, 1975, p. 135.
4) Forrest, M.J. and Peacock, N.J., Plasma Physics Vol. 16, 1974, p. 489.
5) Evans, D.E. and Carolan, P.G., Phys. Rev. Lett. Vol. 25, 1970, p. 1605.
6) Sheffield, J., Plasma Physics Vol. 14, 1972, p. 385.
7) Forrest, M.J., Muraoka, K., and Peacock, N.J., Proc. XIth Conf. Phenomena in Ionized Gases, Prague, 1973.
8) Evans, D.E. and Yeoman, M.L., Phys. Rev. Lett. Vol. 33, 1974, p. 76.
9) Muraoka, K., Hiraki, N., and Kawasaki, S., Rep. Res. Inst. Appl. Mech. Vol. XXII, 1975, p. 177.
10) Evans, D.E. and Katzenstein, J., Rep. Prog. Phys. Vol. 32, 1969, p. 207.
11) Kishimoto, H., Goto, S., and Ito, H., Phys. Rev. Lett. Vol. 18, 1973, p. 1120.
12) Nakagawa, Y. et al, Inst. Plasma Phys., Nagoya Univ. Rep. IPPJ-199, 1974.
13) Watanabe, K. , Private communication.

(Received November 30, 1974)